International Communications in Heat and Mass Transfer 38 (2011) 474–480

Contents lists available at ScienceDirect

International Communications in Heat and Mass Transfer

journal homepage: www.elsevier.com/locate/ichmt

Influence of channel shape on the thermal and hydraulic performance of microchannel heat sink☆

H.A. Mohammed *, P. Gunnasegaran, N.H. Shuaib

Department of Mechanical Engineering, College of Engineering, Universiti Tenaga Nasional, Km7, Jalan Kajang-Puchong, 43009 Kajang, Selangor, Malaysia

ARTICLE INFO

Available online 8 January 2011

Keywords:
Microchannel heat sink (MCHS)
Thermal performance
Zigzag microchannels
Curvy microchannels
Step microchannels

ABSTRACT

Microchannel heat sinks (MCHS) can be made with channels of various shapes. Their size and shape may have remarkable influence on the thermal and hydrodynamic performance of MCHS. In this paper, numerical simulations are carried out to solve the three-dimensional steady and conjugate heat transfer governing equations using the Finite-Volume Method (FVM) of a water flow MCHS to evaluate the effect of shape of channels on the performance of MCHS with the same cross-section. The effect of shape of the channels on MCHS performance is studied for different channel shapes such as zigzag, curvy, and step microchannels, and it is compared with straight and wavy channels. The MCHS performance is evaluated in terms of temperature profile, heat transfer coefficient, pressure drop, friction factor, and wall shear stress. Results show that for the same cross-section of a MCHS, the temperature and the heat transfer coefficient of the zigzag MCHS is the least and greatest, respectively, among various channel shapes. The pressure drop penalty for all channel shapes is higher than the conventional straight MCHS. The zigzag MCHS has the highest value of pressure drop, friction factor, and wall shear stress followed by the curvy and step MCHS, respectively.

1. Introduction

The amount of literature of heat transfer effects on liquid flow in MEMS or in microchannels is vast and growing. In the last two decades, many cooling technologies have been pursued to meet the high heat dissipation rate requirements and maintain a low junction temperature. Among these efforts, the microchannel heat sink (MCHS) has received much attention because of its ability to produce high heat transfer coefficient, small size and volume per heat load, and small coolant requirements. Apart from that, the MCHS cooling concept was first proposed by Tuckerman and Pease [1] in 1981, who pointed out that decreasing liquid cooling channel dimensions to the micron scale will lead to increase in heat transfer rates.

A MCHS is typically contains a large number of parallel microchannels with a hydraulic diameter ranging from 10 to 1000 μm and a coolant is forced to pass through these channels to carry the heat away from a hot surface. Since then, MCHS performances with different types of channel shapes have been studied extensively by many researchers.

Peng and Peterson [2,3] performed experimental investigations on the pressure drop and convective heat transfer for water flow in rectangular straight microchannels. It was found that the cross-sectional aspect ratio had a great influence on the flow friction and convective heat transfer both in laminar and turbulent flows. Philips [4] proposed a method of determining the overall thermal resistance as a function of pertinent variables. He performed a sensitivity analysis to evaluate various parametric effects on his test case and extended the analysis to include larger channel widths of rectangular-shaped microchannels with moderate aspect ratio and for fully developed and developing flows in laminar and turbulent flow regimes. The test sections were fabricated using indium phosphate as the wafer material and water was used as the working fluid. Liu and Garimella [5] conducted flow visualization and pressure drop studies on rectangular straight microchannels with hydraulic diameters ranged from 244 to 974 μm over a Reynolds number range of 230 to 6500. They measured the onset of turbulence through their flow visualization, and they compared their pressure drop measurements with numerical calculations. Their results showed that both conventional turbulent transition and pressure drop correlations are valid on the microscale.

Wu and Cheng [6] studied experimentally the friction factors in smooth trapezoidal silicon straight microchannels with different aspect ratios. They concluded that the *fRe* of liquid flowing in microchannels, having the same hydraulic diameter but with different cross-sectional shapes, can be very much different due to the cross-sectional shape of the channels. Chein and Chen [7] analyzed numerically the fluid flow and heat transfer characteristics in rectangular cross-section MCHS with different inlet/outlet arrangements. They inferred that better performance or uniformities in velocity and temperature can be found in the heat sinks having coolant supply and collection vertically via inlet/outlet ports opened on the heat sink cover plate. Sui et al. [8] reported that significant

☆ Communicated by W.J. Minkowycz.

* Corresponding author.
E-mail address: hussein@uniten.edu.my (H.A. Mohammed).

0735-1933/$ – see front matter © 2010 Elsevier Ltd. All rights reserved.
doi:10.1016/j.icheatmasstransfer.2010.12.031

Nomenclature

A	channel flow area, m^2
c_p	specific heat, J/kg K
D_h	hydraulic diameter, μm ($D_h = 2HW/(H+W)$
f	friction factor, ($f = 2D_h\Delta P/\rho\, u_{in}^2\, L_{ch}$)
$\hat{h}$	dimensionless heat transfer coefficient, ($\hat{h} = h / h_{avg.str.ch.}$)
H	channel height of rectangular, μm
κ	thermal conductivity, W/m K
κ_s	solid thermal conductivity, W/m K
L	straight wavy length, μm
L_c	channel length, μm
n	direction normal to the wall
P	channel wet perimeter, μm
$\hat{P}$	dimensionless pressure drop, ($\hat{P} = \Delta P / \rho u_{in}^2$)
p_{in}	inlet pressure, Pa
p_{out}	outlet pressure, Pa
Q	volume flow rate, m^3/s
q_w	heat flux at microchannel heat sink top plate, W/m^2
Re	Reynolds number, ($Re = \rho\, D_h u_{in}/\mu$)
S	distance between two microchannels, μm
t	substrate thickness, μm
T_{in}	fluid inlet temperature, K
T_s	microchannel heat sink solid temperature, K
u	fluid velocity, m/s
u_{in}	inlet fluid velocity, m/s
U	dimensionless velocity in x-coordinate
V	dimensionless velocity in y-coordinate
W	channel width of rectangular, μm
W	dimensionless velocity in z-coordinate
X, Y, Z	dimensionless Cartesian coordinates

Greek symbols

μ	viscosity, kg/m s
ρ	density, kg/m^3
$\hat{\tau}$	dimensionless wall shear stress, ($\hat{\tau} = \tau / \tau_{avg.str.ch.}$)
θ	dimensionless temperature, ($\theta = T_f - T_i/T_w - T_i$)

Subscripts

avg	average
ch	channel
h	hydraulic
i	inlet
o	outlet
s	solid
str	straight

temperature variations across the chip can persist since the heat transfer performance deteriorates in the flow direction. Moreover, the heat flux in a chip may not be uniform, thus resulting in hot regions which are not easy to be removed using conventional MCHS. These in turn will compromise the reliability of the integrated circuits and can lead to early failures.

It has been well-known that when liquid flows through curved passages, secondary flow (Dean vortices) may be generated which will enhance the stretching and folding of the flow element and thus improves the mixing as well as the heat transfer. This mechanism has been studied by many researchers for heat transfer enhancement [9–12]. Patankar et al. [13] discussed the effect of the Dean vortices on friction factor and heat transfer in the developing and fully developed regions of helically coiled pipes. The effects of the torsion and the Prandtl number were not taken into account. Wang [14] proposed a non-orthogonal helical coordinate system to investigate the effects of curvature and torsion on the low-Reynolds number flow in a helical pipe. Huttl and Friedrich [15,16] studied numerically the effects of curvature and torsion on turbulent flow in helically coiled pipes. The results have shown that the flow quantities were affected by the pipe curvature, whereas the torsion effect was small and it cannot be neglected.

Zheng et al. [17] analyzed numerically the laminar forced convection and thermal radiation in a participating medium inside a helical pipe. The effects of thermal radiation on the convective heat transfer were investigated. They found that the thermal radiation could enhance the total heat transfer rate. Acharya et al. [18] studied numerically the phenomenon of laminar flow, steady heat transfer enhancement in coiled-tube heat exchangers due to chaotic particle paths with two different mixings. A series of correlations of the spatially varying local and constant bulk Nusselt number were presented. Chen and Zhang [19] studied the combined effects of rotation (coriolis force), curvature (centrifugal force), and heating/cooling (centrifugal-type buoyancy force) on the flow and thermal fields. A new concept of chaotic mixing, which relies on changing Dean vortices patterns along the flow direction, was proposed by Schonfeld and Hardt [20] and Jiang et al. [21]. Chaotic advection was generated in a very simple planar channel, which consists of several connected three-quarter circular ducts with curvature changing sign at the connections. This mixing device actually has some similarities to a sinusoidal wavy channel, of which the curvature also changes its sign periodically.

Ngo et al. [22] investigated numerically and experimentally the curvy and zigzag microchannel heat exchanger (MCHE). This study was done to study the thermal performance of MCHE using carbon dioxide and to propose empirical correlations of Nusselt numbers and friction factors. The results show that the Nusselt number of zigzag microchannels is 24–34% higher than that of the curvy microchannels, but the friction factor is, remarkably, four to five times larger depending on the Reynolds number. Zhang et al. [23] performed numerical analysis on the hydrodynamic and thermal characteristics of microchannel networks using finite element method. The simulation model is based on fabricated thick film Low Temperature Co-fired Ceramic (LTCC) substrate with 3D cooling microchannels. A comparison of the cooling performance among step, parallel, and spiral microchannels is also conducted based on the same heat flux and the same flow rate. It was found that step microchannel facilitates the lowest fluid pressure drop and the most uniform temperature distribution over the substrate.

Sun and Jaluria [24,25] developed a parallel numerical algorithm to study the time-dependent characteristics of pressure-driven nitrogen flow in long microchannels under uniform wall heat flux input. Two cases of unsteady convection were studied: the first one arises due to a sudden heat flux change at the channel wall and the second, due to a sudden inlet pressure change. It was found that the transient response for the case with a sudden increase in wall heat flux input is slower than that for the case with a sudden decrease in wall heat flux input. The transient response for the case with a sudden increase in inlet pressure is much faster than that for the case with a sudden decrease in inlet pressure.

Wang et al. [26,27] used the inverse temperature sampling (ITS) to deal with diatomic gaseous flow and heat transfer in a microchannel using the direct-simulation Monte Carlo (DSMC) method. This method was used to calculate the molecular reflective characteristic temperature from the molecular incident energy and the heat flux at the wall boundary. They applied this method to demonstrate the general properties of rarefied diatomic gaseous flow in a microchannel under uniform heat flux boundary conditions and to numerically investigate the effects of wall heat flux on gaseous flow and heat transfer properties. It was concluded that gaseous

rarefication and compressibility increase with the increase of the wall heat flux.

Hong et al. [28] and Zhen et al. [29] simulated the subsonic gas flows through straight rectangular cross-sectional microchannel with patterned microstructures using the direct simulation Monte Carlo (DSMC) method. The 3D microchannel flows are simulated with the cross-section aspect ratio ranging between 1 and 5. The comparison between 3D case and 2D case shows that when the aspect ratio <3, the two extra side walls in the 3D case have significant effects on the heat transfer and flow properties. When the aspect ratio increases, the flow pattern and heat transfer characteristics tend to approach those of 2D results. The microchannel flows with microstructures are also calculated with different Knudsen numbers ranging from 0.08 to 1.8, and with different microstructure temperatures. The results show that the cooling and heating effects of the microstructure temperature on flow properties are enhanced with decreasing Knudsen number.

Chen [30] investigated numerically the effects of temperature-dependent viscosity and thermal conductivity on friction characteristics of incompressible flow in long microchannels involving large temperature variations. It was outlined that their numerical model has fast speed due to the parabolic character of the governing equations and the finite-difference method used. Hong and Asako [31] solved the 2D compressible momentum and energy equations to obtain the heat transfer characteristics of gaseous flows in a microchannel and in a microtube with constant wall temperature. The numerical methodology was based on the arbitrary Lagrangian–Eulerian (ALE) method. Identical heat transfer coefficients were obtained for both cooled and heated cases of incompressible flow. However, in the case of gaseous flow, different heat transfer coefficients were obtained for each cooled and heated case.

It is obvious from the above literature review that the microchannels and microchannels heat sinks were studied extensively but there are very limited researches related to the performance of MCHS with various channel shapes and there are no comprehensive investigations to study the effect of channel shapes on the performance of MCHS. Furthermore, to the best knowledge of the authors, the case of MCHS using different channel shapes has not been given great attention by the researchers in the past and this has motivated the present study. Thus, the objective of this study is to numerically investigate the effect of various channel shapes such as zigzag, curvy, and step MCHS with rectangular cross-section on the overall thermal and hydraulic performance of water flow MCHS. Reynolds number in the range of $100 \le Re \le 1000$ is employed for all channel flow shapes. Results of interest such as temperature profile, heat transfer coefficient, pressure drop, friction factor, and wall shear stress are reported and compared with those of straight and wavy channels with the same cross-section.

2. Mathematical model

The schematic structure of MCHS with zigzag channels is shown in Fig. 1. The details of channels with zigzag, curvy, and step profiles with a constant rectangular cross-section are illustrated in Fig. 2. Heat, supplied to the aluminum MCHS substrate through a top plate, is removed by flowing water through a number of 25 microchannels. The dimensions of all channel shapes with rectangular cross-section are given in Table 1. In this study, the effect of using different channel shapes on heat transfer and fluid flow characteristics of MCHS is considered.

In order to solve the Navier–Stokes and energy equations to investigate the effect of channel shape on the MCHS performance, the following assumptions were made: (i) both fluid flow and heat transfer are in steady state and three dimensional; (ii) fluid is in single phase, incompressible and the flow is laminar; (iii) properties of both fluid and heat sink material are temperature-independent; and (iv) all the surfaces of heat sink exposed to the surroundings are assumed to be insulated except the top plate of heat sink where constant heat flux boundary condition simulating the heat generation from external sources is specified.

The governing equations and its boundary conditions in Cartesian coordinates for 3D laminar incompressible flow for the current problem are [32]:

$$\text{Continuity equation}: \frac{\partial U}{\partial X} + \frac{\partial V}{\partial Y} + \frac{\partial W}{\partial Z} = 0 \tag{1}$$

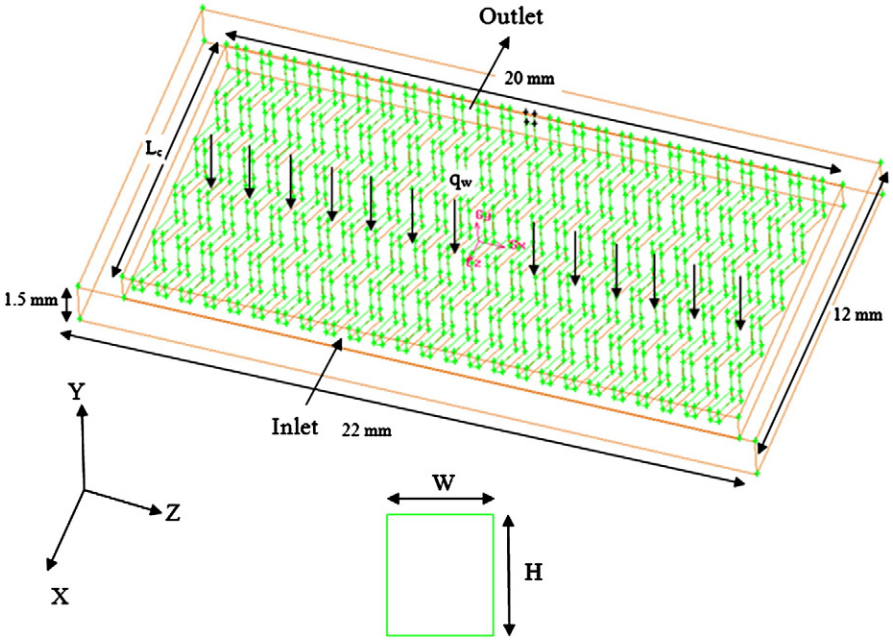

Fig. 1. A schematic diagram of the computational domain of a MCHS.

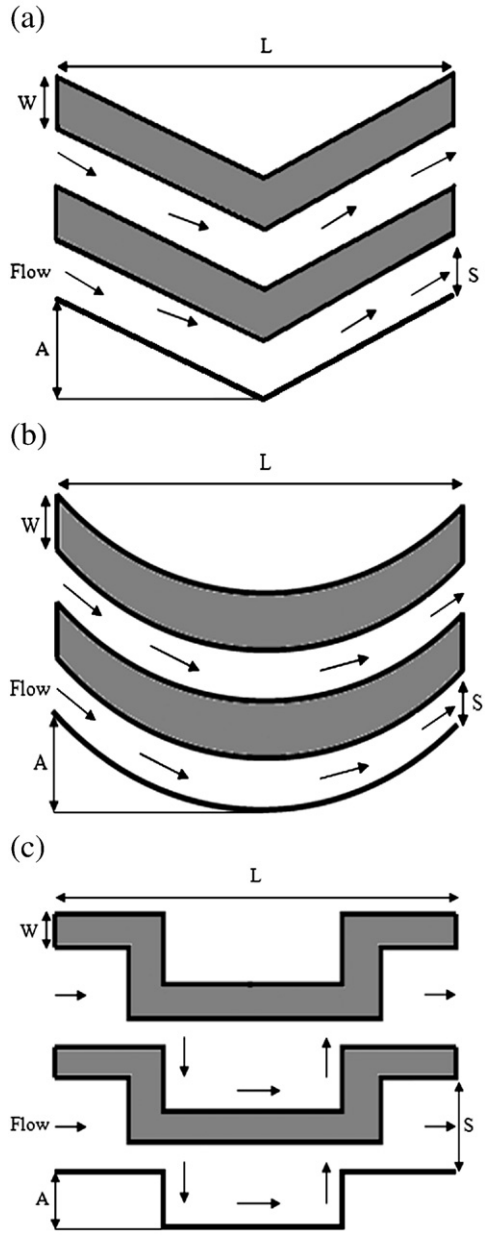

Fig. 2. A schematic of a heat exchange unite with (a) zigzag channels, (b) curvy channels, (c) step channels.

$$\text{X}-\text{Momentum equation}: \left(U\frac{\partial U}{\partial X}+V\frac{\partial U}{\partial Y}+W\frac{\partial U}{\partial Z}\right) = -\frac{\mathrm{d}P}{\mathrm{d}X}+\frac{1}{\mathrm{Re}}\left(\frac{\partial^2 U}{\partial X^2}+\frac{\partial^2 U}{\partial Y^2}+\frac{\partial^2 U}{\partial Z^2}\right) \quad (2)$$

$$\text{Y}-\text{Momentum equation}: \left(U\frac{\partial V}{\partial X}+V\frac{\partial V}{\partial Y}+W\frac{\partial V}{\partial Z}\right) = -\frac{\mathrm{d}P}{\mathrm{d}Y}+\frac{1}{\mathrm{Re}}\left(\frac{\partial^2 V}{\partial X^2}+\frac{\partial^2 V}{\partial Y^2}+\frac{\partial^2 V}{\partial Z^2}\right) \quad (3)$$

Table 1
Geometrical parameters of the MCHS.

D_h (μm)	H (μm)	W (μm)	L (μm)	L_c (μm)	S (μm)
339.15	430	280	2000	10000	500

$$\text{Z}-\text{Momentum equation}: \left(U\frac{\partial W}{\partial X}+V\frac{\partial W}{\partial Y}+W\frac{\partial W}{\partial Z}\right) = -\frac{dP}{dZ}+\frac{1}{\mathrm{Re}}\left(\frac{\partial^2 W}{\partial X^2}+\frac{\partial^2 W}{\partial Y^2}+\frac{\partial^2 W}{\partial Z^2}\right) \quad (4)$$

$$\text{Energy equation}: \left(U\frac{\partial \theta}{\partial X}+V\frac{\partial \theta}{\partial Y}+W\frac{\partial \theta}{\partial Z}\right) = \frac{1}{\mathrm{Re.Pr}}\left(\frac{\partial^2 \theta}{\partial X^2}+\frac{\partial^2 \theta}{\partial Y^2}+\frac{\partial^2 \theta}{\partial Z^2}\right) \quad (5)$$

The dimensionless parameters are:

$$X=\frac{x}{D_h}, Y=\frac{y}{D_h}, Z=\frac{z}{D_h}, U=\frac{u}{D_h}, V=\frac{v}{D_h}, \text{and } W=\frac{w}{u_{in}}$$

At the entrance of the heat sink assembly ($Z=0$, from Fig. 1), two types of boundaries are encountered which are water flows through the microchannels and remove heat conducted to the surface of the heat sink. The remainder of the entrance is occupied by the aluminum substrate. The transverse velocities at the inlet are assumed to be zero. On the aluminum substrate, the velocities are zero, and it is assumed to be an adiabatic surface.

The Boundary conditions used in this study are:

At the inlet:

$$U=1, U=\frac{u}{u_{\text{in}}}, \theta=1$$

At the outlet:

$$P=P_{\text{out}}, \frac{\partial \theta}{\partial n}=0$$

At the fluid-solid interface:

$$U=0, \theta=\theta_s, -k_s\frac{\partial \theta_s}{\partial n}=-k\frac{\partial \theta}{\partial n}$$

At the top plate:

$$q_w=-k_s\frac{\partial \theta_s}{\partial n}$$

By solving the above governing equations along with the boundary conditions using computational fluid dynamic code, the velocity distribution, pressure, and temperature distribution are determined in the fluid and solid domains. From these distributions, one can determine the heat transfer coefficient, pressure drop, friction factor, and wall shear stress. This leads to identify the best channel shape that gives the best thermal and hydraulic performance.

3. Numerical solution and grid independence test

A computational fluid dynamic code is used to calculate flow velocity, pressure, and temperature in the channels of a MCHS. Finite-volume method (FVM) was used to convert the governing equations to algebraic equations accomplished using hybrid differencing scheme [32]. The SIMPLE algorithm was used to enforce mass conservation and to obtain pressure field [33]. This is an iterative solution procedure where the computation is initialized by guessing the pressure field. Then, the momentum equation is solved to determine the velocity components. The pressure is updated using the continuity equation. Even though the continuity equation does not contain any pressure, it can be transformed easily into a pressure correction equation [32]. The segregated solver was used to solve the governing integral equations for the conservation of mass, momentum,

and energy. Because of the assumption of constant fluid thermophysical properties and negligible buoyancy, the mass and momentum equations are not coupled to the energy equation. Therefore, the temperature field is calculated by solving the energy equation after a converged solution for the flow field is obtained by solving the momentum and continuity equations.

A mesh was generated by discretizing the computational domain, and the mesh used is hexahedral cells. For a flow of $Re = 600$, three different number of cells were used. The first cells set was 1.8×10^5, the second cells was 2.9×10^5, and the third cells was 3.7×10^5 in x-, y-, and z-directions for channels and wall, respectively. The computational results for MCHS temperature and heat transfer coefficient for the three meshes are listed in Table 2. Table 2 shows that the solution becomes almost independent of grid size and from second configuration further increase the grids will not have a significant effect on the solution and results of such arrangement are acceptable. Thus, a computational cell with 2.9×10^5 grids is employed throughout the computations in this study. The grid sizes used for curvy, and step channel shapes are the same for zigzag channel shape in the x-, y-, and z-directions. The convergence rate to control the solution for momentum and energy equations were set to be less than 10^{-7}.

4. Results and discussion

For thermal analysis, the fluid used is water with constant properties determined at the mean temperature across the entire length of channels. The inlet temperature of water used as boundary condition is taken as 293 K. The inlet velocity is computed according to the value of Reynolds number, hydraulic diameter, and the properties of fluid. The Reynolds number considered in this work ranged from 100 to 1000. The heat flux that applied at the top plate of MCHS was 100 W/m^2.

4.1. Temperature distribution

The variation of dimensionless average temperature for all channel shapes is presented in Fig. 3. For all channel shapes of MCHS, it is found that the high-temperature region occurs at the edge of the heat sinks since there is no heat dissipation by fluid convection. The low-temperature region occurs in the region where microchannels are placed, especially near the center of the heat sink due to the high heat transfer coefficient as reported in Refs. [7,34,35]. It can clearly be seen from Fig. 3 that the temperature of traditional straight microchannels is the highest among all channel types studied in this work. This may be due to the poor fluid mixing. It is also observed that MCHS with zigzag channel has the lowest value of temperature followed by wavy, curvy, and step channels. From the results obtained, lowest thermal resistance is expected in the zigzag MCHS due to its lowest temperature distribution. Therefore, the zigzag microchannels could greatly enhance the cooling performance of MCHS compared with the traditional straight microchannels.

4.2. Heat transfer coefficient

In straight microchannels, the flow becomes regular and the boundary layer thickens, this causes the heat transfer performance to deteriorate along the flow direction [7,36]. However, zigzag microchannels at moderate Reynolds number generate swirl, eddy, and recirculation flows around their bend corners [22]. For wavy and curvy microchannels, it is found that the Dean vortices can quickly develop along the flow direction and disturb the boundary layer [7,37]. Thus, better heat transfer performance can be expected in zigzag channels, followed by wavy and curvy microchannels. The trend shown in Fig. 4 presents the computed dimensionless average heat transfer coefficient with the number of channels for various channel types at Reynolds number of 600.

It can be seen from Fig. 4 that the middle channel (channel 14) has the highest averaged heat transfer coefficient value. The averaged heat transfer coefficient value for other channels is seen to decrease depending on their distances from the wall. The averaged heat transfer coefficient distribution for all channel shapes of MCHS is almost symmetrical with respect to the centerline of the heat sink. In overall, zigzag channel provides highest heat transfer coefficient compared to

Table 2
Grid independence test.

Mesh configuration	Averaged wall temperature (K)	Averaged Heat transfer coefficient (W/m^2 K)
1.8×10^5	293.39841	8.9118997
2.9×10^5	293.39853	8.9119558
3.7×10^5	293.39861	8.9119984

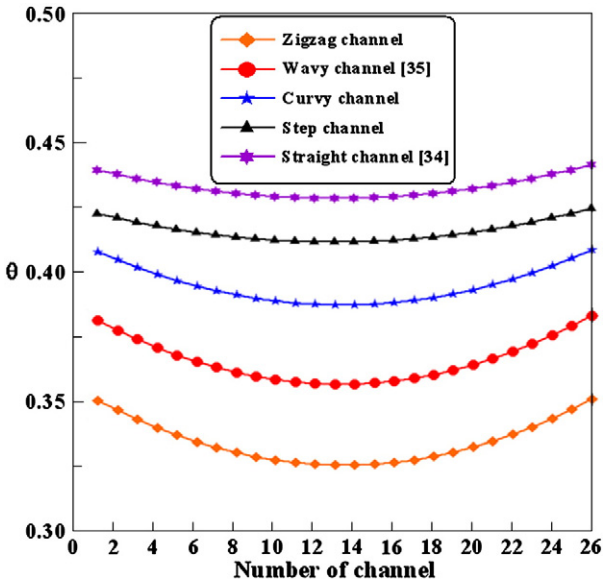

Fig. 3. Dimensionless average temperature profiles with number of channels for different channel shapes ($Re = 600$).

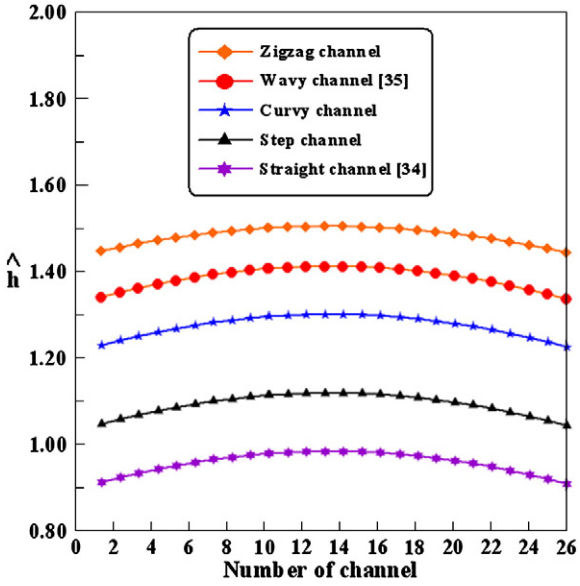

Fig. 4. Dimensionless average heat transfer coefficient with number of channels for different channel shapes ($Re = 600$).

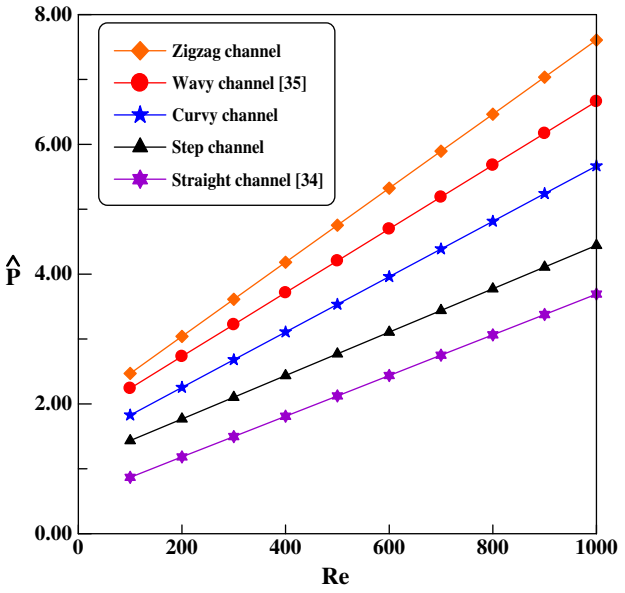

Fig. 5. Variation of pressure drop versus Reynolds number for different channel shapes.

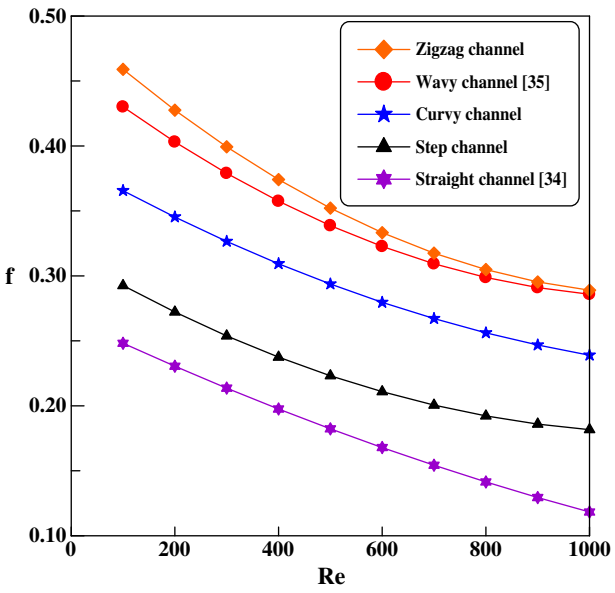

Fig. 6. Variation of friction factor versus Reynolds number for different channel shapes.

other shapes. Although, the heat transfer coefficient of step channel shape is the lowest but it still better than the straight microchannels. This is because the sum of the length of step channels is the longest and the heat transfer area is increased by lengthening the channel [23].

4.3. Pressure drop

The effects of Reynolds number on the pressure drop of various channel shapes with respect to the straight channels are presented in Fig. 5. It can be seen that the pressure drop rises linearly with the increase of Reynolds number. A similar trend is observed for all channel shapes studied. It should be noted that the fluid path in the numerical simulation does not include the fittings and pipes between the pressure transducers used in the actual design of a heat sink. These minor loses increase with fluid kinetic energy, which it is proportional to the square of Reynolds number. It is clearly observed that the variation of pressure drop for all channel shapes is higher than the straight channels as reported by Sui et al. [8]. The zigzag microchannels have the highest value of pressure drop and followed by wavy and curvy microchannels, respectively. The zigzag flow channel configuration generates swirl, eddy, and recirculation flows around their bend corners, thereby resulting in large pressure drop. The step channels have the lowest pressure drop penalty among others channel shapes. This difference is mainly attributable to the difference in flow channel configuration. In contrast, the wavy and curvy flow channels configuration causes neither swirl, eddies, nor recirculation flow but generates the Dean vortices which cause the secondary flows [7,36,38]. This engenders lower pressure drop than zigzag channels but higher than step channels.

4.4. Friction factor

The variation of the friction factor with Reynolds number for various channel shapes is shown in Fig. 6. The results show that the friction factor decreases with the increase of Reynolds number for all channel shapes. It can be inferred that the changing of Dean vortices patterns along the flow direction through the wavy and curvy channels appears to give an increase in the friction factor compared to step and straight channels for all values of Reynolds number. However, it is found that the friction factor of zigzag channels is still higher than that of the wavy and curvy channels. This trend is also reported by Refs. [7,22].

4.5. Wall shear stress

The effect of using various channel shapes on the local dimensionless wall shear stress is also investigated and presented in Fig. 7. In general, for all cases examined, the highest wall shear stress is observed in zigzag channels due to the largest pressure drop as discussed in the previous section. It can also be noticed that the wall shear stress of zigzag channels is patterned in fluctuating form with constant amplitude. While the wall shear stress of wavy and curvy channels also appeared in fluctuating form, it decreases because the amplitude is decreased along the flow direction. The wall shear stress of step and straight channels decreases linearly along the flow direction. This phenomenon may be attributed to the changing of secondary flow patterns along the

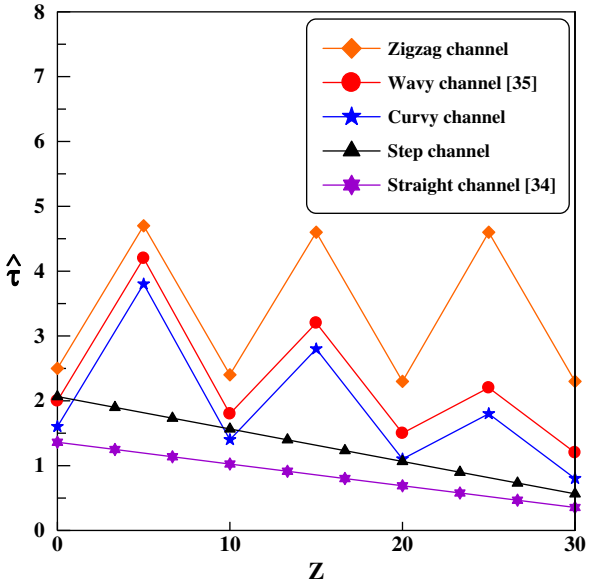

Fig. 7. Variation of dimensionless wall shear stress along the length of flow direction for different channel shapes.

flow direction and the complex interaction between Dean vortices and channel wall, which disturbs the fluid path in the zigzag, wavy and curvy channels.

5. Conclusions

In this paper, numerical simulations are made to study the effect of channel shape on the thermal and flow fields of water flow in MCHS. Three different channel shapes are considered zigzag, curvy, and step MCHS, and it is compared with straight and wavy MCHS. From the results, it is concluded that:

1. The temperature and the heat transfer coefficient of the zigzag MCHS is the least and greatest, respectively, among other channel shapes studied. The second best thermal performance is provided by curvy channels after the wavy channels.
2. The pressure drop penalty for all channel shapes of MCHS is higher than the conventional straight MCHS.
3. The zigzag MCHS has the highest value of pressure drop, friction factor, and wall shear stress followed by the wavy, curvy and step MCHS, respectively.
4. Thus, the zigzag MCHS is the best channel for the best thermal performance and the step MCHS is the best channel for the hydraulic performance with moderate degradation of heat transfer compared to conventional straight MCHS.

Acknowledgements

The authors would like to sincerely thank the Ministry of Higher Education (MOHE) of Malaysia for the provision of a small grant with code no FRGS01090010 to support this work.

References

[1] D.B. Tuckerman, R.F. Pease, High performance heat sinking for VLSI, IEEE Electron. Devices Lett. EDL 2 (1981) 126–129.
[2] X.F. Peng, G.P. Peterson, The effect of thermofluid and geometrical parameters on convection of liquids through rectangular microchannels, Int. J. Heat Mass Transfer 38 (1995) 755–758.
[3] X.F. Peng, G.P. Peterson, Convective heat transfer and flow friction for water flow in microchannels structures, Int. J. Heat Mass Transfer 39 (1996) 2599–2608.
[4] R.J. Philips, Forced-convection, liquid-cooled microchannel heat sinks, Master Thesis, Massachusetts Institute of Technology, Cambridge, MA, 1987.
[5] D. Liu, S.V. Garimella, Investigation of liquid flow in microchannels, J. Thermophys Heat Transfer 18 (2004) 65–72.
[6] H.Y. Wu, P. Cheng, Friction factors in smooth trapezoidal silicon microchannels with different aspect ratios, Int. J. Heat Mass Transfer 46 (2003) 2519–2525.
[7] R. Chein, J. Chen, Numerical study of the inlet/outlet arrangement effect on microchannel heat sink performance, Int. J. Therm. Sci. 48 (2009) 1627–1638.
[8] Y. Sui, C.J. Teo, P.S. Lee, Y.T. Chew, C. Shu, Fluid flow and heat transfer in wavy microchannels, Int. J. Heat Mass Transfer 53 (2010) 2760–2772.
[9] C.E. Kalb, J.D. Seader, Heat and mass transfer phenomena for viscous flow in curved circular tubes, Int. J. Heat Mass Transfer 15 (4) (1972) 801–817.
[10] J.H. Masliyah, K. Nandakumar, Fully developed viscous flow and heat transfer in curved semi-circular sectors, AIChE J. 25 (3) (1979) 478–487.
[11] L. Wang, T. Yang, Bifurcation and stability of forced convection in curved ducts of square cross-section, Int. J. Heat Mass Transfer 47 (2004) 2971–2987.
[12] G. Yang, Z.F. Dong, M.A. Ebadian, Laminar forced convection in a helicoidal pipe with fine pitch, Int. J. Heat Mass Transfer 38 (5) (1995) 853–862.
[13] S.V. Patankar, V.S. Pratap VS, D.B. Spalding, Prediction of laminar flow and heat transfer in helically coiled pipes, J. Fluid Mech. 62 (1) (1974) 35–51.
[14] C.Y. Wang, On the low-Reynolds number flow in a helical pipe, J. Fluid Mech. 108 (1) (1981) 85–94.
[15] T.J. Huttl, R. Friedrich, Influence of curvature and torsion on turbulent flow in helically coiled pipes, Int. J. Heat Fluid Flow 21 (3) (2000) 45–53.
[16] T.J. Huttl, R. Friedrich, Direct numerical simulation of turbulent flows in curved and helically coiled pipes, Comput. Fluids 30 (2001) 591–605.
[17] B. Zheng, C.X. Lin, M.A. Ebadian, Combined laminar forced convection and thermal radiation in helical pipe, Int. J. Heat Mass Transfer 43 (10) (2000) 67–78.
[18] N. Acharya, M. Sen, H.C. Chang, Analysis of heat transfer enhancement in coiled-tube heat exchangers, Int. J. Heat Mass Transfer 44 (31) (2001) 89–99.
[19] H. Chen, B. Zhang, Fluid flow and mixed convection heat transfer in a rotating curved pipe, Int. J. Therm. Sci. 42 (10) (2003) 47–59.
[20] F. Schönfeld, S. Hardt, Simulation of helical flows in microchannels, AIChE J. 50 (2004) 771–778.
[21] F. Jiang, K.S. Drese, S. Hardt, M. Küpper, F. Schönfeld, Helical flows and chaotic mixing in curved microchannels, AIChE J. 50 (2004) 2297–2305.
[22] T.L. Ngo, Y. Kato, K. Nikitin, T. Ishizuka, Heat transfer and pressure drop correlations of microchannel heat exchangers with S-shaped and zigzag fins for carbon dioxide cycles, Exp. Therm. Fluid Sci. 32 (2007) 560–570.
[23] J. Zhang, Y.F. Zhang, M. Miao, Y.F. Jin, S.L. Bai, J.Q. Chen, Simulation of fluid flow and heat transfer in microchannel cooling for LTCC electronic packages, IEEE Electronic Packaging Technology and High Density Packaging, ICEPT-HDP 9, 2009, pp. 327–330.
[24] Z. Sun, Y. Jaluria, Unsteady two-dimensional nitrogen flow in long microchannels with uniform wall heat flux, Numer. Heat Transf. A 57 (9) (2010) 625–641.
[25] Z. Sun, Y. Jaluria, Numerical modeling of pressure-driven nitrogen slip flow in long rectangular microchannels, Numer. Heat Transf. A 56 (7) (2009) 541–562.
[26] Q.W. Wang, C.L. Zhao, M. Zeng, Y.N. Wu, numerical investigation of rarefied diatomic gas flow and heat transfer in a microchannel using DSMC with uniform heat flux boundary condition—part I: numerical method and validation, Numer. Heat Transf. B 53 (2) (2008) 160–173.
[27] Q.W. Wang, C.L. Zhao, M. Zeng, Y.N. Wu, Numerical investigation of rarefied diatomic gas flow and heat transfer in a microchannel using DSMC with uniform heat flux boundary condition—part II: applications, Numer. Heat Transf. B 53 (2) (2008) 174–187.
[28] Z.C. Hong, C.E. Zhen, C.Y. Yang, Fluid dynamics and heat transfer analysis of three dimensional microchannel flows with microstructures, Numer. Heat Transf. A 54 (3) (2008) 293–314.
[29] C.E. Zhen, Z.C. Hong, Y.J. Lin, N.T. Hong, Comparison of 3-D and 2-D DSMC heat transfer calculations of low-speed short microchannel flows, Numer. Heat Transf. A 52 (3) (2007) 239–250.
[30] C.S. Chen, Reduced Navier–Stokes simulation of incompressible microcahnnel flows, Numer. Heat Transf. A 53 (1) (2008) 71–87.
[31] C. Hong, Y. Asako, Heat transfer characteristics of gaseous flows in a microchannel and a microtube with constant wall temperature, Numer. Heat Transf. A 52 (3) (2007) 219–238.
[32] S.V. Patankar, Numerical Heat Transfer and Fluid Flow, Hemisphere, New York, 1980.
[33] J.D. Anderson, Computational Fluid Dynamic: The Basics with Applications, McGraw-Hill, New York, 1995.
[34] P. Gunnasegaran, H.A. Mohammed, N.H. Shuaib, R. Saidur, The effect of geometrical parameters on heat transfer characteristics of microchannels heat sink with different shapes, Int. Commun. Heat Mass Transfer 37 (8) (2010) 1078–1086.
[35] H.A. Mohammed, P. Gunnasegaran, N.H. Shuaib, Numerical simulation of heat transfer enhancement in wavy microchannel heat sink, Int. Commun. Heat Mass Transfer 38 (1) (2011) 63–68.
[36] S. Kandlikar, S. Garimella, D. Li, S. Colin, M.R. King, Heat Transfer and Fluid Flow in Minichannels and Microchannels, Elsevier, USA, 2005.
[37] E. Utriainen, B. Sunden, Numerical analysis of primary surface trapezoidal cross wavy duct, Int. J. Numer. Method Heat Fluid Flow 10 (6) (2000) 634–648.
[38] W. Yang, J. Zhang, H. Cheng, The study of flow characteristics of curved microchannel, Appl. Therm. Eng. 25 (2010) 1894–1907.